Interaction of KCNE subunits with the KCNQ1 K^+ channel pore

Gianina Panaghie[1,2], Kwok-Keung Tai[3] and Geoffrey W. Abbott[1,2]

[1] *Greenberg Division of Cardiology, Department of Medicine and* [2] *Department of Pharmacology, Cornell University, Weill Medical College, 520 East 70th Street, New York, NY 10021, USA*

[3] *The Parkinson's and Movement Disorder Research Laboratory, Long Beach Memorial Medical Center, 2625 Pasadena Avenue, Long Beach, CA 90806, USA*

KCNQ1 α subunits form functionally distinct potassium channels by coassembling with KCNE ancillary subunits MinK and MiRP2. MinK-KCNQ1 channels generate the slowly activating, voltage-dependent cardiac I_{Ks} current. MiRP2-KCNQ1 channels form a constitutively active current in the colon. The structural basis for these contrasting channel properties, and the mechanisms of α subunit modulation by KCNE subunits, are not fully understood. Here, scanning mutagenesis located a tryptophan-tolerant region at positions 338–340 within the KCNQ1 pore-lining S6 domain, suggesting an exposed region possibly amenable to interaction with transmembrane ancillary subunits. This hypothesis was tested using concomitant mutagenesis in KCNQ1 and in the membrane-localized 'activation triplet' regions of MinK and MiRP2 to identify pairs of residues that interact to control KCNQ1 activation. Three pairs of mutations exerted dramatic effects, ablating channel function or either removing or restoring control of KCNQ1 activation. The results place KCNE subunits close to the KCNQ1 pore, indicating interaction of MiRP2-72 with KCNQ1-338; and MinK-59,58 with KCNQ1-339, 340. These data are consistent either with perturbation of the S6 domain by MinK or MiRP2, dissimilar positioning of MinK and MiRP2 within the channel complex, or both. Further, the results suggest specifically that two of the interactions, MiRP2-72/KCNQ1-338 and MinK-58/KCNQ1-340, are required for the contrasting gating effects of MinK and MiRP2.

(Resubmitted 24 October 2005; accepted after revision 17 November 2005; first published online 24 November 2005)
Corresponding author G. W. Abbott: Starr 463, Greenberg Division of Cardiology, Weill Medical College of Cornell University, 520 East 70th Street, New York, NY 10021, USA. Email: gwa2001@med.cornell.edu

KCNQ1 is a voltage-gated potassium α subunit that forms tetrameric complexes in the plasma membrane to selectively conduct potassium ions (Wang *et al.* 1996*b*; Yang *et al.* 1997). While homomeric KCNQ1 channels are functional, it has become increasingly evident that at least some of the physiological functions of KCNQ1 require its coassembly with single transmembrane domain ancillary subunits from the MinK-related peptide (MiRP) family, encoded by *KCNE* genes. In human heart, KCNQ1 associates with MinK (*KCNE1*) to form the cardiac I_{Ks} channel that contributes to ventricular repolarization (Barhanin *et al.* 1996; Sanguinetti *et al.* 1996). Channels formed by coassembly of KCNQ1 with MiRP2 (*KCNE3*) generate a potassium current thought to regulate cAMP-stimulated intestinal chloride secretion in the colon (Schroeder *et al.* 2000).

KCNE subunits interact promiscuously with a range of voltage-gated potassium channel α subunits including KCNQ1, hERG, and members of the Kv1, Kv2, Kv3 and Kv4 subfamilies; and with hyperpolarization-activated HCN channels, that pass both K^+ and Na^+ ions (McCrossan & Abbott, 2004). KCNQ1 is the only α subunit known to interact with all five cloned KCNE subunits in heterologous expression studies (Barhanin *et al.* 1996; Sanguinetti *et al.* 1996; Schroeder *et al.* 2000; Tinel *et al.* 2000; Angelo *et al.* 2002; Grunnet *et al.* 2002, 2005; Teng *et al.* 2003). The most-studied KCNQ1 interactions are with MinK and MiRP2, which have dramatic and distinct effects on KCNQ1 gating. MinK slows and right-shifts KCNQ1 activation, increases unitary conductance and removes inactivation (Barhanin *et al.* 1996; Sanguinetti *et al.* 1996; Sesti & Goldstein, 1998; Yang & Sigworth, 1998). MiRP2 greatly reduces the voltage dependence of KCNQ1 leading to a largely voltage-independent potassium 'leak' current, also appearing to lack inactivation (Schroeder *et al.* 2000; Abbott & Goldstein, 2002).

Several pieces of evidence indicate that MinK and MiRP2 interact with the KCNQ1 pore, and that specific residues within the MinK and MiRP2 transmembrane domains impact KCNQ1 gating. First, accessibility of

 DOI: 10.1113/jphysiol.2005.100644

introduced cysteines in MinK to Cd^{2+} and MTS reagents suggests that MinK residues lie close to the I_{Ks} pore and selectivity filter (Wang *et al.* 1996*a*; Tai *et al.* 1997; Tai & Goldstein, 1998). Second, by constructing chimeras between MinK and MiRP2, Melman and colleagues identified an 'activation triplet' region within the transmembrane domains of MinK and MiRP2, the central amino-acid within the triplet being implicated as the major gating determinant in complexes with KCNQ1 (Melman *et al.* 2001, 2002). Third, co-immunoprecipitation of chimeric α subunits with MinK and MiRP2 demonstrated physical interaction of these KCNE peptides with the potassium channel pore-lining regions, and in particular the S6 domain (Melman *et al.* 2004). These previous studies suggested that residues in the MinK and MiRP2 transmembrane domains – and specifically within the 'activation triplets' – might influence gating by interaction within the KCNQ1 pore. Recently, however, it was argued that while the MiRP2 activation triplet actively modulates KCNQ1 activation, the equivalent domain in MinK is passive, revealing gating controlled by the MinK C-terminal domain (Gage & Kobertz, 2004).

Interacting points between α subunits and KCNE peptides are sought after because while high-resolution structures of several potassium channel α subunits have been determined (Doyle *et al.* 1998; Jiang *et al.* 2002, 2003; Long *et al.* 2005), high-resolution structures of α-KCNE co-complexes are not yet known. Thus, we understand relatively little about how KCNE peptides can fit within an apparently tightly packed α subunit tetramer, or the structural basis for the impact of KCNE peptides on voltage-gated potassium channel pharmacology, which is important given their value as therapeutic targets.

Here, using tryptophan-scanning mutagenesis of the KCNQ1 S6 domain we identified a relatively 'tolerant' region at residues 338–340. Subsequent coexpression with MinK and MiRP2 'activation triplet' mutants pinpointed specific residue-to-residue interactions with the tryptophan-tolerant region of KCNQ1. The new data suggest a model in which MinK and MiRP2 reside in slightly different positions close to the KCNQ1 pore, or alternatively that they each perturb the S6 helix differently. Further, they suggest that the transmembrane regions of both MinK and MiRP2 contribute to controlling KCNQ1 activation.

Methods

Molecular biology

hKCNQ1, hMinK and hMiRP2 mutants were constructed using the QuickChange Multi Site-Directed Mutagenesis Kit (Stratagene). The mutated genes were sequenced in their entirety to confirm appropriate mutations and check for inadvertent mutations, then subcloned into oocyte expression vectors. hKCNQ1 was cloned into a pBluescript-based vector, and MinK and MiRP2 were cloned into pRAT (Bockenhauer *et al.* 2001). cRNA transcripts were produced from *Not*I-linearized DNA templates using the T3 (KCNQ1) and T7 (MiRPs) mMessage mMachine kits (Ambion). cRNA was quantified by spectrophotometry and its size integrity verified by gel electrophoresis. Stage V and VI *Xenopus laevis* oocytes were purchased from Nasco (Fort Atkinson, WI, USA). Oocytes were defolliculated with collagenase type I (Gibco, Grand Island, NY, USA) then injected with approximately 10 ng of α subunit cRNA alone or with 2 ng of MinK or MiRP2 cRNA.

Electrophysiology

Whole-cell currents in oocytes were recorded at room temperature by two-electrode voltage clamp (TEVC) using an OC-725C Amplifier (Warner Instruments, CT, USA) and an IBM computer. Pipettes were filled with 3 M KCl and had a 0.4–1.5 MΩ resistance. Bath solution was (mM): 4 KCl, 96 NaCl, 0.7 $MgCl_2$, 1 $CaCl_2$, 10 Hepes (pH 7.6 with NaOH). Experiments were performed 3–4 days after cRNA injection. Oocytes were held at −80 mV, stepped for 3 s at voltages between −120 and +60 mV in 20 mV steps, then held for 1–2 s at −30 mV before returning to the holding potential.

Data analysis

Current–voltage relationships were obtained by measuring current at the time point of peak current for positive voltage steps, typically at the end of 3 s depolarizing pulses but nearer the start of the pulse in the case of rapidly inactivating mutants. Current–voltage relationships were either fitted with a straight line, or with a sigmoidal fit using the Boltzman equation ($G = G_{max}/[1 + \exp(V - V_{½}/k)]$, where $V_{½}$ is the half-maximal activation, and k is the slope factor. For rise times to half-maximal current, 'maximal' was the peak current observed during the 3 s depolarizing pulse. Data analysis was performed using CLAMPFIT 9 (Axon Instruments) and tabulated in Excel 5.0. Graphs were generated using Origin 6.0. Data are expressed as mean ± S.E.M., with n specifying the number of independent experiments. Statistical analysis was performed with Sigma Stat 2.0 and statistical significance was assumed if $P < 0.05$ as calculated using the Mann-Whitney Rank sum test.

Results

A tryptophan-tolerant region in the KCNQ1 pore

Tryptophan-scanning mutagenesis has previously been employed to identify tolerant regions within

membrane proteins that do not pack closely with other transmembrane domains, but instead face lipid or dead-space (Monks *et al.* 1999; Hong & Miller, 2000). Here, tryptophan-scanning mutagenesis of the KCNQ1 pore-lining S6 domain was undertaken to identify tryptophan-tolerant residues that might face lipid or dead-space in homomeric KCNQ1 channels, and thus potentially accommodate interaction with MinK or MiRP2 upon their coassembly with KCNQ1. Residues 336–345 of the KCNQ1 S6 domain were chosen because of their predicted position in the KCNQ1 pore based on homology to the bacterial K^+ channel KcsA, for which a high-resolution structure has been solved (Doyle *et al.* 1998) (Fig. 1*A*). Further, A336 in KCNQ1 is an equivalent position to the glycine hinge of the MthK bacterial potassium channel (Jiang *et al.* 2002), and KCNQ1-G345 is part of the noted PXP motif (actually PXG in KCNQ1 α subunits) that is thought to induce a kink in the S6 of most voltage-gated potassium channels (Del Camino *et al.* 2000).

Functional analysis of the 10 KCNQ1 tryptophan mutants, using TEVC of oocytes injected with wild-type or mutant KCNQ1 cRNA, revealed that only S338W, F339W and F340W channels were functional, demonstrating a relatively confined tryptophan-tolerant pocket in the KCNQ1 pore (Fig. 1*B*). This discovery was striking because a previous cysteine scan of the KCNQ1 S6 domain had identified these three residues as important for interaction with KCNE peptides, although the specific KCNE residues with which each of the three KCNQ1 positions interacted were not determined (Melman *et al.* 2004).

Effects of tryptophan substitutions at position 338–340 on KCNQ1 gating

Two of the three functional tryptophan mutants – S338W and F339W – had similar voltage-dependent activation to wild-type KCNQ1, though S338W significantly reduced the peak current amplitude of homomeric channels (Figs 1*B* and 2). In contrast, F340W channels showed predominantly constitutive (voltage-independent) activation (Fig. 2), passing significant inward current at hyperpolarized potentials, as is the case for wild-type MiRP2-KCNQ1 complexes (Fig. 3). All three functional mutants also exhibited increased inactivation compared to wild-type KCNQ1 channels suggesting that this region of the channel is also important in KCNQ1 inactivation (Fig. 2*A*), but in the present study analysis is focused upon effects on activation.

The KCNE peptides MinK and MiRP2 regulate multiple aspects of KCNQ1 channel function. Specifically, MinK slows KCNQ1 activation, eliminates KCNQ1 inactivation (Fig. 3*A*), and increases KCNQ1 unitary conductance 4-fold (Barhanin *et al.* 1996; Sanguinetti *et al.* 1996; Sesti & Goldstein, 1998; Tristani-Firouzi & Sanguinetti, 1998; Yang & Sigworth, 1998). MiRP2 converts KCNQ1 to a predominantly constitutively open channel; MiRP2-KCNQ1 channels do not appear

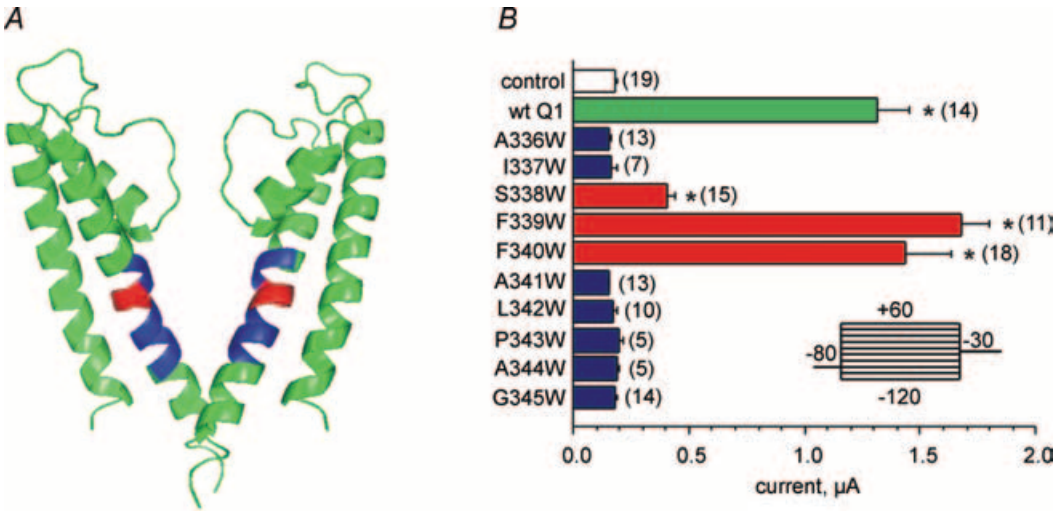

Figure 1. Tryptophan scanning of the KCNQ1 S6 domain
A, position of the 10 KCNQ1 S6 residues mutated to tryptophan, according to their corresponding residues on the bacterial K^+ channel KcsA. Green, non-mutated; blue, non-functional when mutated to tryptophan; red, functional when mutated to tryptophan. *B*, mean peak current of control (water-injected) oocytes, and oocytes expressing wild-type or tryptophan-mutant KCNQ1 channels. Currents were recorded by TEVC at +40 mV using a standard voltage family protocol (inset); *n* values indicated on right. Error bars indicate S.E.M.; *significant difference from control current, $P < 0.05$. Colour coding as in *A*.

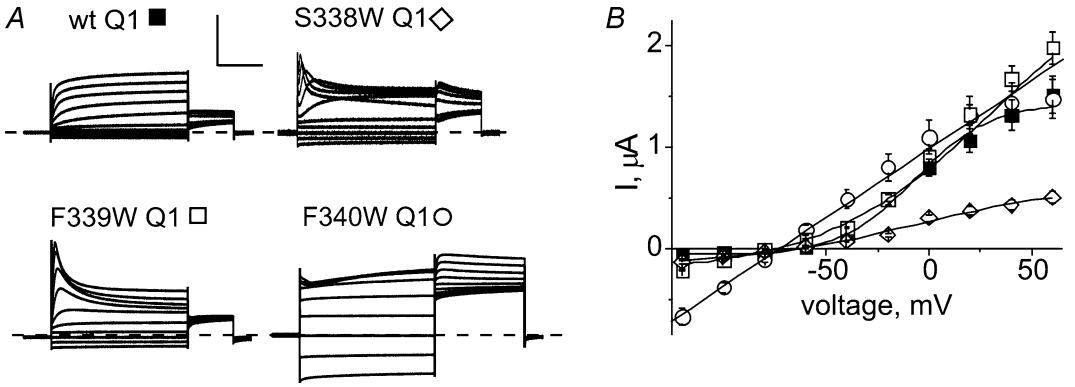

Figure 2. Gating effects of tryptophans at KCNQ1 residues 338–340
A, exemplar current traces recorded in oocytes expressing wild-type or tryptophan mutant KCNQ1 (Q1) channels as indicated. Currents were recorded by TEVC using the standard voltage family protocol as in Fig. 1. Scale bars: vertical, 1 μA except 0.4 μA for S338W-KCNQ1; horizontal, 1 s. Zero current level indicated by dashed line. *B*, mean peak *I–V* relationship for oocytes as in *A*; $n = 11$–18. Error bars indicate S.E.M.

to undergo any significant inactivation (Fig. 3*A–C*) (Schroeder *et al.* 2000). The phenomenon of constitutive activation is easily apparent in exemplar traces (Fig. 3*A*, bottom left trace), or can be quantified by constructing an *I–V* curve, showing a distinctive near-linear *I–V* relationship (Fig. 3*B*). Alternatively, a bar graph of peak current at −120 mV as a fraction of peak current at +60 mV can be used to distinguish constitutive from voltage-dependent activation in a range of channel types, as voltage-dependent Kv channels are not opened by stepping to −120 mV (Fig. 3*C*).

Previously, the McDonald laboratory defined the 'activation triplet', a contiguous series of residues within the transmembrane domain of MinK (57–59) and equivalent residues in MiRP2 (71–73) affecting KCNQ1 gating; the central residue of each triplet in particular was

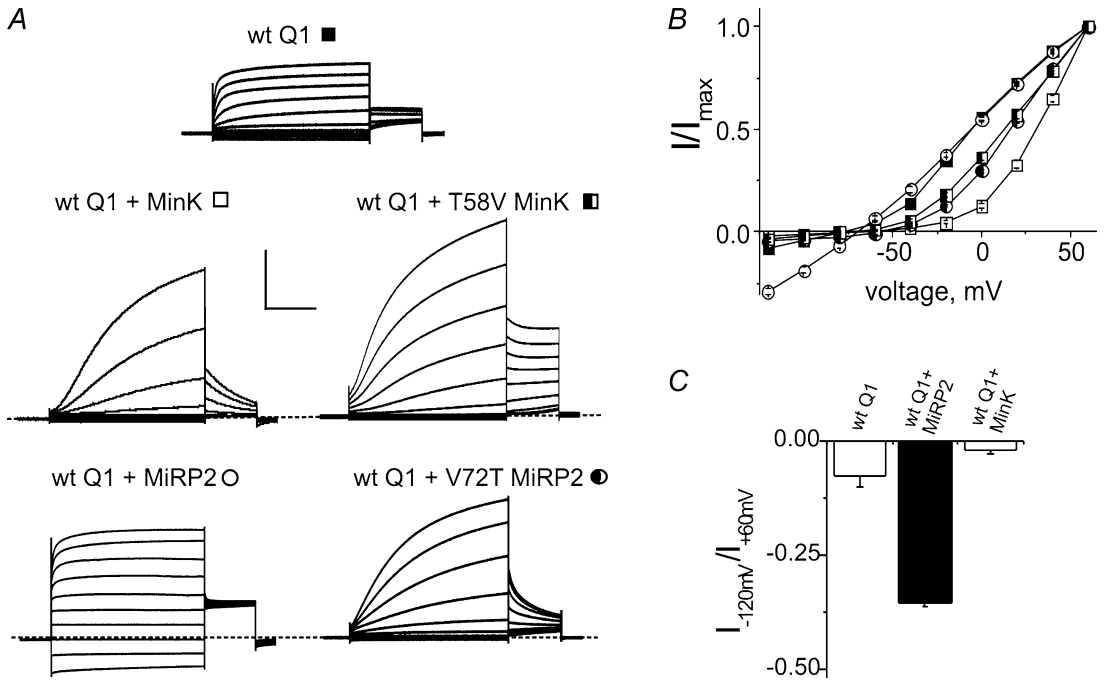

Figure 3. Gating effects of wild-type and mutant MinK and MiRP2 on wild-type KCNQ1
A, exemplar current traces recorded in oocytes expressing wild-type (wt) KCNQ1 alone or with wt or mutant MinK or MiRP2, as indicated. Currents were recorded by TEVC using the voltage family protocol as in Fig. 1. Scale bars, 2 μA, except for wt KCNQ1 (1 μA); and 1 s. Zero current level indicated by dashed line. *B*, Mean peak *I–V* relationship for oocytes; symbols as in *A*; $n = 6$–14. Error bars indicate S.E.M. *C*, normalized constitutive current at −120 mV for oocytes injected with wt KCNQ1 alone or with wt MinK or MiRP2 as indicated.

found to influence activation (Melman *et al.* 2001, 2002). Here, we recapitulated their reported effects of replacing the central residue in the MiRP2 activation triplet with that of MinK, showing that V72T-MiRP2-KCNQ1 channels activate like MinK-KCNQ1 rather than MiRP2-KCNQ1 channels (Fig. 3*A* and *B*). Results with the reciprocal swap, i.e. inserting the central MiRP2 activation triplet residue into MinK (creating T58V), showed that while T58V-MinK still endowed some slow, voltage-dependent activation on KCNQ1, these mixed channels also exhibited some constitutive current at positive voltages, and tended to stay open during the −30 mV tail pulse, once opened with depolarized voltages (Fig. 3*A*). Melman and colleagues observed that the function of channels formed from this combination of subunits is conditional, varying with holding potential, conditioning pulses, and duration of interpulse intervals (Melman *et al.* 2001, 2002). Our observations are consistent with these previous findings since here the T58V-MinK-KCNQ1 channels only partially deactivate during the −30 mV tail pulse (after activation at positive prepulse voltages), with the majority remaining open at a voltage which deactivates wild-type MinK-KCNQ1 channels.

Having recapitulated the effects of mutant MinK and MiRP2 on wild-type KCNQ1, we next combined mutagenesis and functional analysis of coexpressed KCNQ1 and MinK or MiRP2 to determine specific KCNE–KCNQ1 interaction points that coordinate control of KCNQ1 activation. Since tryptophan substitutions at position 338–340 themselves introduce changes in homomeric KCNQ1 channel gating, we draw our conclusions by comparing the effects of mutant MinK or MiRP2 to the effects of wild-type MinK or MiRP2 on the respective KCNQ1 S6 mutant channel. Activation phenotype is the principal criterion in interpreting our results with slow, voltage-dependent activation being the hallmark for complexes containing wild-type MinK and constitutive current at all voltages being the hallmark for complexes containing wild-type MiRP2.

Interaction of KCNQ1 S338 variants with wild-type and mutant MinK and MiRP2

Injection of MinK cRNA into oocytes generates a slowly activating I_{Ks}-like current by coassembly with endogenous oocyte KCNQ1 (Takumi *et al.* 1988; Sanguinetti *et al.* 1996). This coassembly is usurped by coexpressed wild-type human KCNQ1, favouring formation of all-human I_{Ks} complexes (Chen *et al.* 2003) (Fig. 3*A*). Injection of MiRP2 cRNA alone into oocytes does not generate currents significantly different from water-injected oocytes (Schroeder *et al.* 2000). Here, the KCNQ1-like activation and increased inactivation of homomeric S338W-KCNQ1 channels (Fig. 2) were replaced with slower, I_{Ks}-like activation and loss of inactivation upon coexpression with wild-type human MinK, demonstrating that MinK regulated S338W-KCNQ1 activation and inactivation as with wild-type KCNQ1 (Fig. 4*A* and *B*). Swapping 'activation triplet' residues between MinK and MiRP2 and coexpressing each of these mutants with S338W-KCNQ1 showed that all three mutant forms of MinK gated essentially as wild-type MinK forming heteromeric complexes that exhibited wild-type I_{Ks}-like activation (Fig. 4*A* and *B*) with little constitutive current (Fig. 4*D*) and a relatively slow rise-time to half-maximal current of around 1 s (Fig. 4*E*). These data indicate that interaction with S338 is not essential for modulation of KCNQ1 activation by residues in the MinK 'activation triplet'.

Wild-type MiRP2 was able to regulate S338W-KCNQ1 activation as normal, producing predominantly constitutively open channels (Fig. 4*A*) with a near-linear *I–V* relationship (Fig. 4*C*), prominent inward currents at −120 mV (Fig. 4*D*), and an instantaneous rise to half maximal current (Fig. 4*E*), similar to those seen with wild-type MiRP2-KCNQ1 complexes (Fig. 3). T71F and G73L mutant forms of MiRP2 also formed predominantly constitutively active channels with S338W-KCNQ1 (Fig. 4*A*, *C*, *D* and *E*). In contrast, V72T-MiRP2 exerted no functional effects on S338W-KCNQ1 activation (Fig. 4*A*), did not produce a linear *I–V* relationship (Fig. 4*C*) and showed little current at −120 mV (Fig. 4*D*). Note that the V72T-MiRP2 variant is functionally active because it was able to modulate wild-type KCNQ1 activation (Fig. 3) and also it significantly decreased the normalized peak tail current of channels formed with S338W-KCNQ1, especially after more negative prepulses (Fig. 4*C* inset). These data suggested that KCNQ1 S338 coordinates control of activation via MiRP2 V72.

To further investigate this hypothesis, we performed reciprocal mutagenesis, creating S338T-KCNQ1 and V72W-MiRP2, and coexpressed them. The lack of constitutive current, and *G–V* relationship (measured from tail currents), of both homomeric S338T channels and S338T-KCNQ1/wild-type MiRP2 channels closely matched that of S338T-V72W channels (Supplementary Fig. 1*A* and *B*). An assessment of inactivation, quantified as steady-state current compared to peak current, showed that inactivation is less extensive in S338T-V72W channels than in homomeric S338T-KCNQ1 channels, confirming that S338T forms complexes with V72W-MiRP2 (Supplementary Fig. 1*C*). As neither wild-type nor V72W-MiRP2 alter S338T activation we conclude that the effects of the S338T mutation override effects of MiRP2 on activation, indicating the importance of this KCNQ1 position in coordinating gating effects of MiRP2. This does not provide additional evidence directly supporting interaction specifically with MiRP2 position 72, which we infer from results

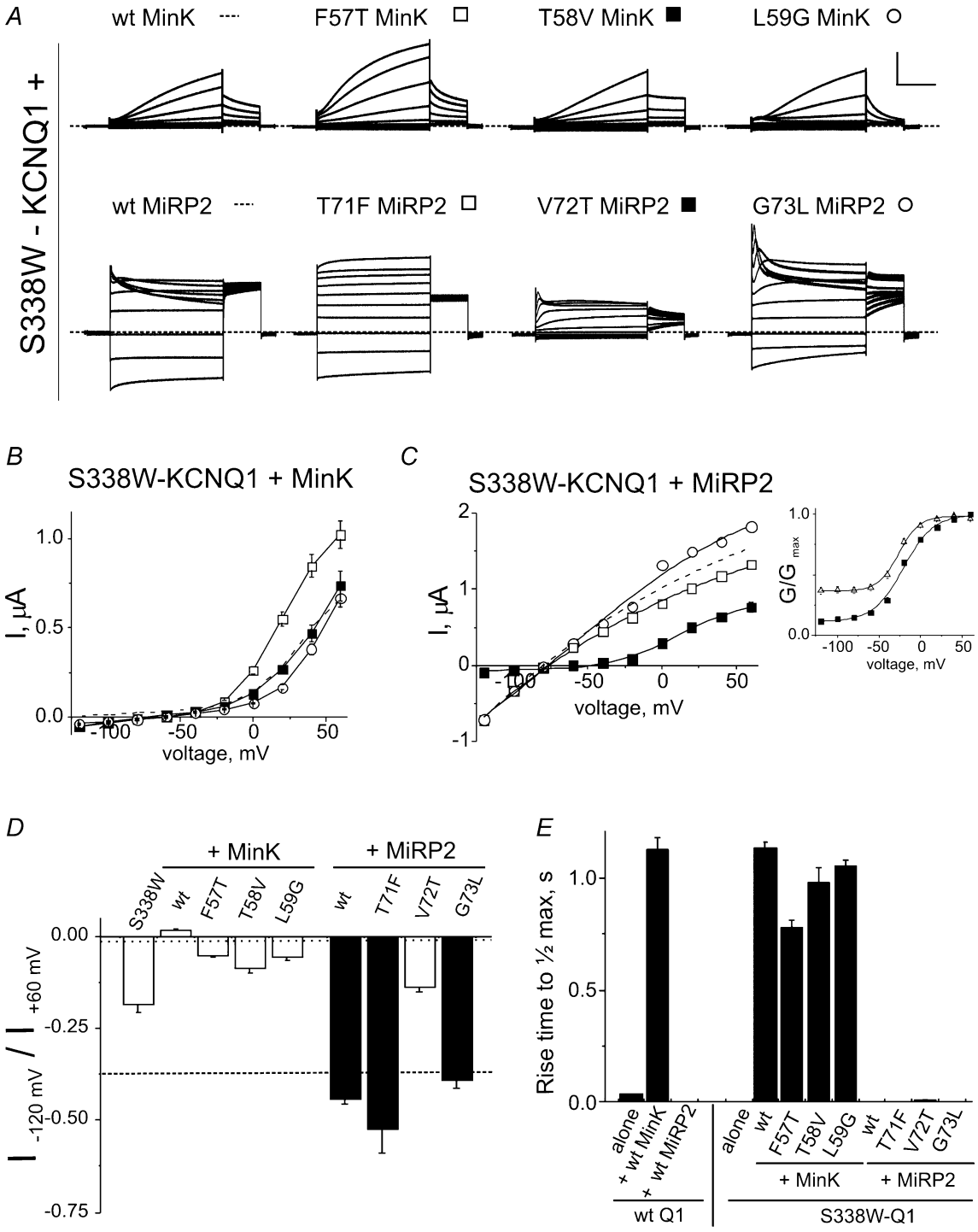

Figure 4. Interaction of S338W-KCNQ1 with MinK and MiRP2
A, exemplar current traces recorded in oocytes expressing S338W-KCNQ1 with wild-type (wt) or mutant MinK or MiRP2, as indicated. Currents were recorded by TEVC using the standard voltage family protocol as in Fig. 1. Scale bars, 0.5 μA and 1 s. Zero current level indicated by dashed line. *B*, mean peak *I–V* relationships for oocytes injected with S338W-KCNQ1 and MinK variants; symbols as in *A*; $n = 10$–17. Error bars indicate S.E.M. *C*, mean peak *I–V* relationships for oocytes injected with S338W-KCNQ1 and MiRP2 variants; symbols as in *A*; $n = 9$–15. Error bars indicate S.E.M. Inset: a normalized *G–V* curve for S338W-KCNQ1 alone (△) and S338W + V72T-MiRP2 (■). *D*, normalized constitutive current at −120 mV for oocytes injected as indicated. Dotted line indicates wt KCNQ1 + wt MinK; dashed line indicates wt KCNQ1 + wt MiRP2 as in Fig. 3 for comparison. *E,* activation kinetics expressed as time to reach half-maximal current for oocytes injected as indicated.

obtained from S338W-V72T channels (Fig. 4*A*). However, additional experiments examining the coexpression of wild-type KCNQ1 with V72W-MiRP2 provide additional support for the importance of MiRP2 V72 in influencing KCNQ1 gating, since these channels exhibited predominantly slowly activating, non-constitutive current more reminiscent of wild-type MinK-KCNQ1 complexes, albeit with a shorter rise-time to half-maximal current due to some constitutive current (Supplementary Fig. 1*D*). Further, our conclusion that KCNQ1 S338 is not critical for modulation by MinK is strongly supported by the observation that coexpression of S338T-KCNQ1 with wild-type MinK results in typical MinK-KCNQ1-like slow, non-constitutive activation with a rise-time to half-maximal current of ∼1 s (Supplementary Fig. 1*D*).

Interaction of F339W-KCNQ1 with wild-type and mutant MinK and MiRP2

F339W-KCNQ1 formed homomeric channels with voltage-dependent activation similar to wild-type KCNQ1, but with increased inactivation (Fig. 2). Wild-type MinK formed slowly activating, non-inactivating channels with F339W-KCNQ1, similar to wild-type I_{Ks} in that they exhibited no constitutive current (Fig. 5*A* and *B*) and displayed a rise-time to half-maximal current close to 1 s, similar to wild-type MinK-KCNQ1 (Fig. 5*E*). Thus wild-type MinK tolerated a tryptophan at position 339 on KCNQ1. Coexpression of F339W-KCNQ1 with MinK carrying MiRP2 'activation triplet' substitutions showed that channels formed with F57T-MinK and T58V-MinK also generated slow-activating, voltage-dependent I_{Ks} currents (Fig. 5*A*, *B* and *E*). In contrast, L59G-MinK + F339W-KCNQ1 heteromeric channels were non-functional (Fig. 5*A*). We often observed a small outward current in oocytes expressing these channels when the membrane was depolarized to +60 mV; however, this current did not exhibit the slow kinetics of activation characteristic to MinK-containing complexes, nor was it sensitive to HMR1556, a specific inhibitor of the I_{Ks} current (data not shown). Thus we conclude that this small current did not arise from heterologously expressed F339W-KCNQ1. As L59G-MinK is functionally expressed and does not exert a dominant negative effect on the other KCNQ1 mutants tested, and as F339W-KCNQ1 was functional alone or with the seven other MinK or MiRP2 (see below) variants tested, the non-functionality of F339W-L59G channels suggests disruption of a specific functional interaction between L59-MinK and F339-KCNQ1, or alternatively adoption of a novel, non-functional interaction (see below).

Wild-type MiRP2 did not override the effects of the F339W mutation in KCNQ1 to produce significant constitutive current, nor did any of the three MiRP2 activation triplet mutants tested; all complexes were, however, functional (Fig. 5*A*, *C* and *E*). An analysis of inactivation rates for F339W-KCNQ1 channels with and without wild-type MiRP2, however, demonstrated the two can interact because MiRP2 significantly slowed inactivation rate 22–36% depending on voltage (Fig. 5*D*). Thus the absence of effects of MiRP2 on F339W-KCNQ1 activation is specific for this process, and not indicative of a loss of physical interaction or lack of influence upon other gating processes. Indeed, T71F-MiRP2 up-regulated KCNQ1 current 6-fold, due at least in part to greatly reduced inactivation (Fig. 5*A*), but did not convert KCNQ1 to a leak channel or alter the normalized current–voltage relationship (Fig. 5*C* and *E*).

The data suggest that F339 in KCNQ1 interacts with MinK via residue L59, as a glycine in the latter position is tolerated by the other KCNQ1 variants tested. No interactions between MiRP2 and F339 in KCNQ1 were suggested in the control of activation, although it is clear that F339W-KCNQ1 subunits physically interact with MiRP2 variants, and it is certainly possible that F339 and MiRP2-T71 interact to regulate inactivation, a line of future investigation outside the scope of this study. Interestingly, Melman and colleagues found that F339C-KCNQ1 channels produce no current in combination with wild-type MiRP2 (Melman *et al.* 2004), while we found that F339W was tolerated by all MiRP2 variants. Another interpretation of our finding that F339W-KCNQ1/L59G-MinK channels are non-functional could be that this combination actually produces an interaction that does not normally exist – one which locks the channel in a non-conducting or closed state. This might be visualized as KCNQ1 residue 339 normally swinging by position 59 in MinK (or similar residue in MiRP2) during the transition from closed to open. With the 339W–59G combination, this transition may be prevented because of formation of a preternatural, stable interaction between the two mutant residues; this may also happen in MiRP2-KCNQ1 channels, but only when a cysteine occupies the 339 position (Melman *et al.* 2004).

Interaction of F340W-KCNQ1 with wild-type and mutant MinK and MiRP2

Homomeric F340W-KCNQ1 channels showed predominantly constitutive activation, reminiscent of wild-type MiRP2-KCNQ1 channels, but also exhibited some inward rectification due to voltage-dependent inactivation (Fig. 2*A* and *B*). Channels formed with wild-type MinK and F340W-KCNQ1 were constitutively open, as apparent from exemplar traces (Fig. 6*A*), *I–V* relationships (Fig. 6*B*), relative current at −120 mV (Fig. 6*D*) and rise-time to half-maximal current (Fig. 6*E*).

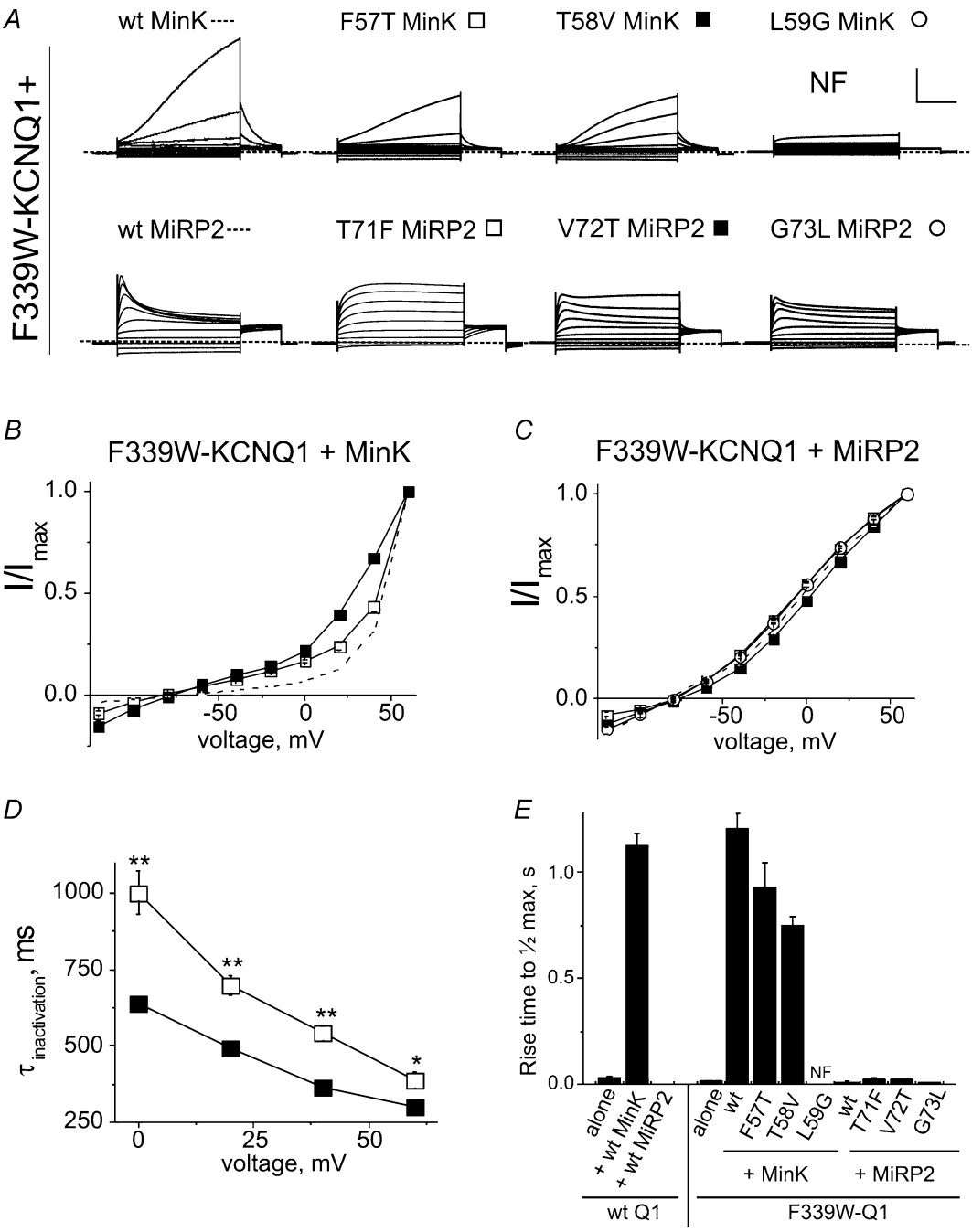

Figure 5. Interaction of F339W-KCNQ1 with MinK and MiRP2
A, exemplar current traces recorded in oocytes coexpressing F339W-KCNQ1 with wild type (wt) or mutant MinK or MiRP2, as indicated. Currents were recorded by TEVC using the standard voltage family protocol as in Fig. 1. Scale bars: vertical, 1 μA except 2 μA for F339W-KCNQ1 + wt MinK and 6 μA for F339W-KCNQ1 + T71F-MiRP2; horizontal, 1 s. Zero current level indicated by dashed line. NF, non-functional. *B*, mean normalized peak *I–V* relationships for oocytes coinjected with F339W-KCNQ1 and MinK variants; symbols as in *A*; $n = 6$–9. Error bars indicate S.E.M. *C*, mean normalized peak *I–V* relationships for oocytes coinjected with F339W-KCNQ1 and MiRP2 variants; symbols as in *A*; $n = 8$–9. Error bars indicate S.E.M. *D*, inactivation time constants for F339W- KCNQ1 alone (■) and F339W-KCNQ1 + wt MiRP2 (□) obtained by fitting the current at indicated voltages to a monoexponential function. Asterisks indicate statistically significant difference between the two groups (*$P < 0.01$; **$P < 0.001$). *E*, activation kinetics expressed as time to reach half-maximal current for oocytes injected as indicated.

These channels also exhibited inward rectification and current decay at more depolarized voltages, again due to voltage-dependent inactivation (Fig. 6*A* and *B*). Thus, channels formed by wild-type MinK with F340W-KCNQ1 show tail currents of equal current magnitude irrespective of prepulse voltage, as expected for a conductance set entirely by driving force and not by the voltage dependence of activation (Fig. 6*A*).

Two of the MinK mutant variants bearing MiRP2 'activation triplet' residues – F57T and L59G – produced channels closely resembling those formed with wild-type MinK, i.e. constitutively active but with voltage-dependent inactivation (Fig. 6*A*, *B*, *D* and *E*). In striking contrast, T58V-MinK was able to restore I_{Ks}-like slow, voltage-dependent activation in channels formed with F340W-KCNQ1 (Fig. 6*A*, *D* and *E*), giving a characteristic outwardly rectifying *I–V* relationship (Fig. 6*B*).

Neither wild-type nor mutant MiRP2 significantly altered the *I–V* relationship of the largely constitutively active current observed in complexes formed with F340W-KCNQ1 (Fig. 6*A*, *C* and *D*), therefore showing an instantaneous rise to half-maximal current (Fig. 6*E*). Since the F340W mutation essentially acts as a surrogate for MiRP2, eliciting constitutive activation in KCNQ1 channels, one might argue that this is not a surprising result. However, if F340 were important for coordinating the gating effects of MiRP2, then it might be possible to disrupt its effects by introducing a MinK residue into the MiRP2 activation triplet, as was observed albeit in reverse with MinK T58V (Fig. 6*A*, upper). These data therefore suggest against functional interaction of position 340 with residues in MiRP2 to influence KCNQ1 activation.

Thus, MinK position 58 was the single example out of eight MinK or MiRP2 variants that altered F340W-KCNQ1 activation, with the T58V substitution appearing to compensate for the F340W substitution. One possible interpretation of these data is a tolerance of the tryptophan at position 340 for the small, hydrophobic valine on MinK position 58, but an intolerance for the similarly sized but polar (hydroxyl-bearing) threonine. Attempts to study the reciprocal mutations, F340V-KCNQ1 with T58W-MinK, were unfortunately thwarted by the non-functionality of F340V-KCNQ1 alone or with any MinK variants tested (data not shown).

Discussion

The discovery of a relatively tryptophan-tolerant region in the KCNQ1 S6 domain led to the hypothesis that this constitutes either a region of flexibility or that these residues face lipid or dead-space in homomeric KCNQ1 channels. The existence of this region in the midst of the KCNQ1 potassium channel pore suggested these three residues might potentially accommodate interaction with residues from transmembrane ancillary peptides MinK and MiRP2, possibly because this region is exposed on the outer face of S6. This tolerance is admittedly limited: in wild-type KCNQ1 residues 339 and 340 are phenylalanines – aromatic but lacking the prominent indole ring of tryptophan, the largest of all naturally occurring amino acid side chains – and all three substitutions lead to substantial changes in KCNQ1 function. We conclude that the other, non-functional tryptophan mutants identify residues closely juxtaposed with other KCNQ1 regions such as the S5 or other membrane-spanning helices, resulting in non-functional channels, or misfolding and consequent disruption of normal trafficking to the cell surface.

Double mutagenesis between the tryptophan-tolerant region in KCNQ1 and the 'activation triplet' region of MinK and MiRP2 produced highly specific effects on channel gating. Only one out of a total of eight KCNE variants (wild-type and three mutant forms each for MinK and MiRP2) showed significant effects with each KCNQ1 tryptophan mutant examined. V72T-MiRP2 was the only variant to not tolerate the S338W substitution in KCNQ1. F339W-L59G channels were the only non-functional complexes of all 24 combinations studied employing the KCNQ1 338–340 tryptophan mutations. The F340W–T58V combination was the only example in which I_{Ks}-like activation was reinstated by MinK mutagenesis when not present with wild-type MinK.

Results of a prior study employing MiRP2 truncation mutants suggested a refinement of the 'activation triplet' model, namely that while the MiRP2 transmembrane domain is an active determinant of activation, the MinK transmembrane domain is passive, allowing control of gating by the MinK C-terminal region (Gage & Kobertz, 2004). Results in the current study are certainly consistent with an active MiRP2 transmembrane domain. In S338W-KCNQ1 channels, none of the MinK mutants disenabled MinK from conferring slow, voltage-dependent activation, whereas mutation of position 72 in MiRP2 disrupted the constitutive activation conferred by wild-type MiRP2. In terms of a role of the MinK 'activation triplet' in actively controlling gating *versus* merely capitulating to effects of the C-terminal domain, consider data derived from KCNQ1 F339W and F340W mutants. In F339W channels, those formed with L59G-MinK were non-functional. This supports the importance of F339–L59 interaction in creating functional channel complexes, but does not necessarily assert that this interaction controls activation. On the other hand, F340W-KCNQ1 channels, which were constitutively active in their homomeric form, exhibited slow, voltage-dependent activation only when coassembled with T58V-MinK. This not only supports close juxtaposition of T58 and F340, but also suggests

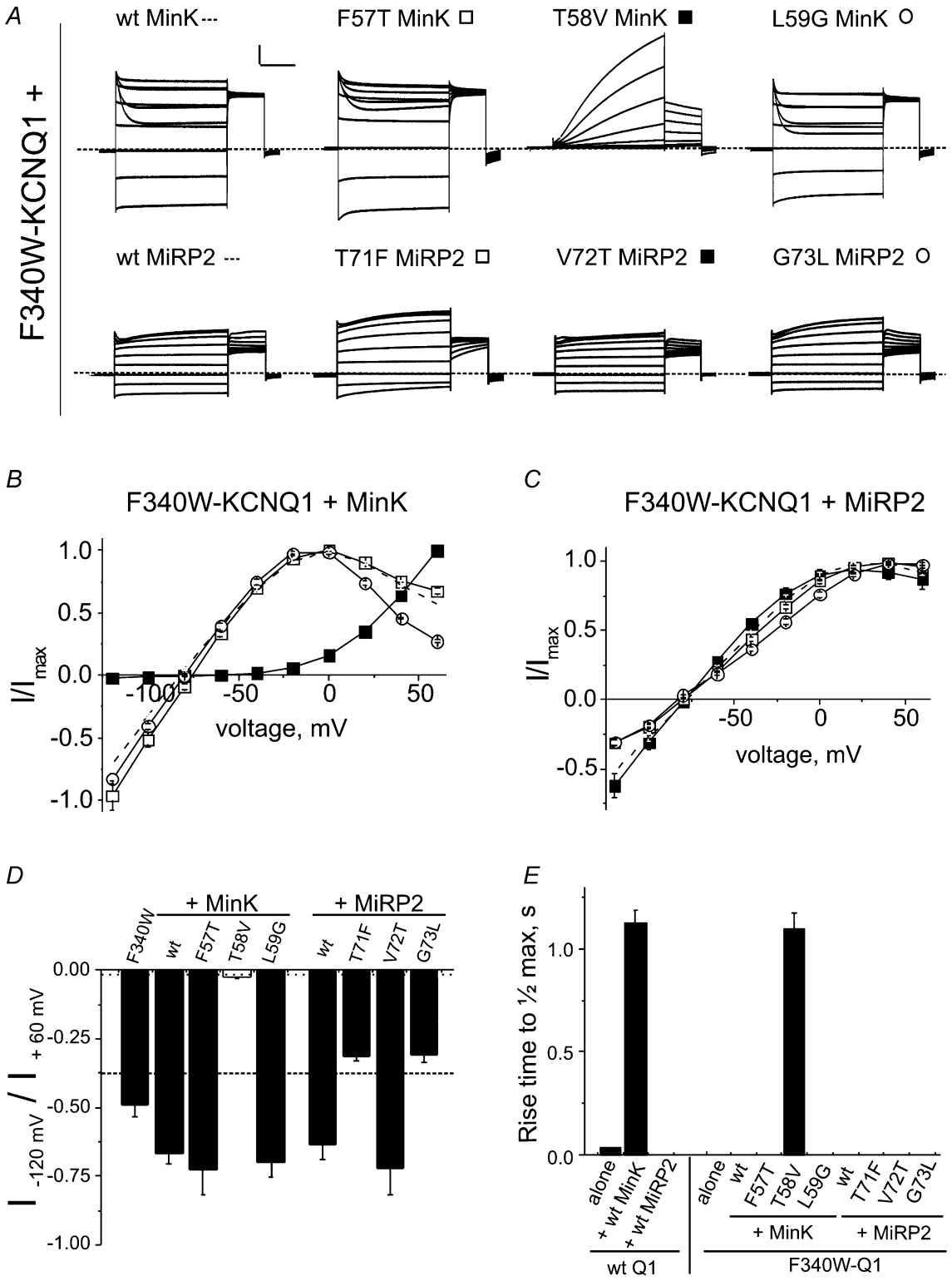

Figure 6. Interaction of F340W-KCNQ1 with MinK and MiRP2
A, exemplar current traces recorded in oocytes expressing F340W-KCNQ1 with wild- type (wt) or mutant MinK or MiRP2, as indicated. Currents were recorded by TEVC using the standard voltage family protocol as in Fig. 1. Vertical scale bar: 0.5 μA except 1 μA for L59G-MinK, wt MiRP2 and T71F-MiRP2 and 2 μA for T58V-MinK. Horizontal scale bar: 1 s. Zero current level indicated by dashed line. *B*, mean normalized peak *I–V* relationships for oocytes coinjected with F340W-KCNQ1 and MinK variants; symbols as in *A*; $n = 4$–12. Error bars indicate S.E.M. *C*, mean

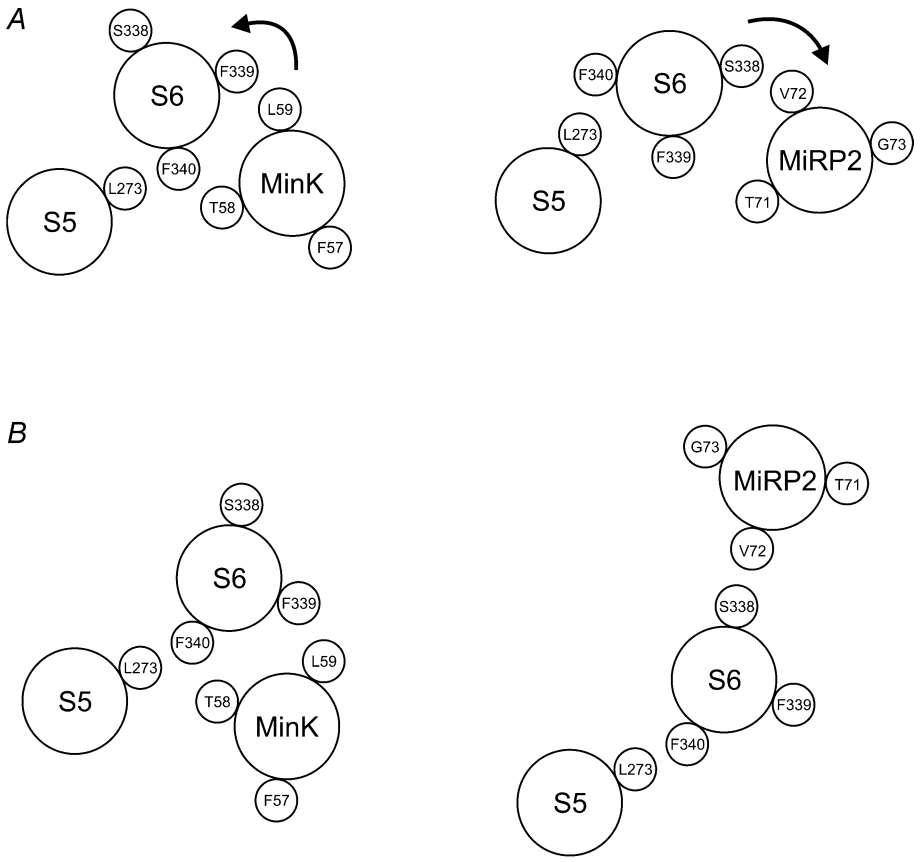

Figure 7. Possible positions of MinK and MiRP2 within the KCNQ1 pore
Cartoons derived from helical wheel projections showing possible positions of KCNQ1 S5, S6 domains and MinK or MiRP2 transmembrane domains, based upon functional effects of mutants described in this study and in Seebohm *et al.* (2005). *A*, in this model, MinK or MiRP2 perturb the S6 domain but the relative distances between the central axes of S5, S6 and MinK or MiRP2 are similar. *B*, an alternative model in which S6 is not perturbed by MinK or MiRP2, each of which adopt different positions in the pore.

that the valine at position 58 directly influences the activation of T58V–F340W complexes. The ability of T58V in MinK to override effects of the F340W mutant is difficult to reconcile with the model of a passive MinK transmembrane domain.

The new data, while useful as an indication of the molecular determinants influencing activation in KCNE–KCNQ1 complexes, can also be used to construct a simple structural model of KCNE–KCNQ1 interaction points. Recently, Seebohm and colleagues proposed that F340 in the KCNQ1 S6 domain interacts with L273 in the KCNQ1 S5 domain, based on functional studies of double mutant KCNQ1 channels (Seebohm *et al.* 2005). This observation, together with results of the current study and previous work showing that the MinK transmembrane domain is predominantly α-helical (Mercer *et al.* 1997), suggest two alternative models for positioning of MinK and MiRP2 relative to the KCNQ1 S5 and S6 domains (Fig. 7). In the first model, MinK and MiRP2 each perturb S6 in a different fashion, but the relative positions of the centres of the S5, S6 and either MinK or MiRP2 transmembrane helices are the same in either case (Fig. 7*A*). This model would seem to be the most likely, given the overall similarity between MinK and MiRP2. However, during activation gating the S6 domain is thought to undergo significant movements including both angular and rotational movements, involving the region encompassing KCNQ1 residues 338–340 (Jiang *et al.* 2002). It is possible therefore that during activation different S6 residues (such as 338 and 340) are closer to the residing KCNE subunit at different times, and that the differences in interaction points we observed

normalized peak *I–V* relationships for oocytes coinjected with F340W-KCNQ1 and MiRP2 variants; symbols as in *A*; $n = 7$–14. Error bars indicate S.E.M.*D*, normalized constitutive current at −120 mV for oocytes injected as indicated. Dotted line indicates wt KCNQ1 + wt MinK; dashed line indicates wt KCNQ1 + wt MiRP2 as in Fig. 3 for comparison. *E*, activation kinetics expressed as time to reach half-maximal current for oocytes injected as indicated.

in this study reflect the tendency of MinK or MiRP2 to stabilize different conformational states of the S6 during the activation process. In this scenario, there are no differences between the relative positioning of the S6 and KCNE helices during the gating process, but MinK or MiRP2 each halt or influence the S6 movement at different stages during activation, stabilizing contrasting states and leading to the functional differences observed upon their coexpression with KCNQ1. This model was previously suggested by others (Melman *et al.* 2004) and is certainly highly consistent with data in the present study. A second model, considered less likely given the high degree of overall similarity between the MinK and MiRP2 transmembrane domains, is that the position of the KCNQ1 S6 domain relative to MinK is significantly different than the predicted position with respect to MiRP2, but the relative S5–S6 positioning is preserved (Fig. 7*B*).

Any study employing mutagenesis combined with functional assays to draw conclusions about interaction points between proteins must be approached with caution because of the difficulties in interpreting functional effects in terms of structure, but this has been a widely employed technique in the channel field, because of the absence until relatively recently of direct structural evidence. We still lack direct evidence of the structure of KCNE–α subunit complexes, and understand relatively little about how KCNE subunits can intercalate into α subunit tetramers to modulate channel function. The data here provide a hypothetical picture of KCNE placement with respect to the pore-lining S6 helix, but do not specify when during the gating process these pairs might interact.

The data also provoke several further questions into the mechanisms by which MiRP2 endows KCNQ1 with constitutive activation, a little-understood phenomenon with wide-ranging physiological implications. First, while our results suggest a precise MiRP2–KCNQ1 interaction point that influences activation, they do not explain how this single interaction point can achieve such a dramatic change in channel behaviour. Second, in contrast to its effects on activation, wild-type MiRP2 did not remove the atypically extensive, voltage-dependent inactivation of S338W-KCNQ1 channels, which notably remained despite predominantly voltage-independent activation (Fig. 4*A*). In fact, T71F-MiRP2 was the only MiRP2 variant able to remove inactivation in S338W-KCNQ1 channels, perhaps suggesting that different MiRP2 residues regulate KCNQ1 activation *versus* inactivation (Fig. 4*A*). Third, the ability of 340W to bestow constitutive activation upon KCNQ1 channels, with or without MiRP2 (Figs 2*A* and 6*A*), may indicate that the extra indole group at position 340 perturbs the local S6 domain conformation in a similar fashion to MiRP2. It does not, however, provide direct evidence of interaction between MiRP2 and KCNQ1 residue 340, nor does it shed light on how perturbation of S6 can lock KCNQ1 channels in the open state.

In summary, we present evidence of functional interaction between specific MinK and MiRP2 'activation triplet' residues with specific residues in the KCNQ1 S6 domain. The data refine current models of α–KCNE subunit juxtaposition and suggest two alternatives for positioning of MinK and MiRP2 in the KCNQ1 pore. These models are probably salient for other α–KCNE complexes, and support suggestions by others that KCNE peptides are positioned close to residues that form the ion conduction pathway of voltage-gated potassium channels (Tai & Goldstein, 1998; Melman *et al.* 2004).

References

Abbott GW & Goldstein SA (2002). Disease-associated mutations in KCNE potassium channel subunits (MiRPs) reveal promiscuous disruption of multiple currents and conservation of mechanism. *Faseb J* **16**, 390–400.

Angelo K, Jespersen T, Grunnet M, Nielsen MS, Klaerke DA & Olesen SP (2002). KCNE5 induces time- and voltage-dependent modulation of the KCNQ1 current. *Biophys J* **83**, 1997–2006.

Barhanin J, Lesage F, Guillemare E, Fink M, Lazdunski M & Romey G (1996). K_VLQT1 and lsK (minK) proteins associate to form the I_{Ks} cardiac potassium current. *Nature* **384**, 78–80.

Bockenhauer D, Zilberberg N & Goldstein SA (2001). KCNK2: reversible conversion of a hippocampal potassium leak into a voltage-dependent channel. *Nat Neurosci* **4**, 486–491.

Chen H, Sesti F & Goldstein SA (2003). Pore- and state-dependent cadmium block of I_{Ks} channels formed with MinK-55C and wild-type KCNQ1 subunits. *Biophys J* **84**, 3679–3689.

Del Camino D, Holmgren M, Liu Y & Yellen G (2000). Blocker protection in the pore of a voltage-gated K^+ channel and its structural implications. *Nature* **403**, 321–325.

Doyle DA, Morais Cabral J, Pfuetzner RA, Kuo A, Gulbis JM, Cohen SL, Chait BT & MacKinnon R (1998). The structure of the potassium channel: molecular basis of K^+ conduction and selectivity. *Science* **280**, 69–77.

Gage SD & Kobertz WR (2004). KCNE3 truncation mutants reveal a bipartite modulation of KCNQ1 K^+ channels. *J General Physiol* **124**, 759–771.

Grunnet M, Jespersen T, Rasmussen HB, Ljungstrom T, Jorgensen NK, Olesen SP & Klaerke DA (2002). KCNE4 is an inhibitory subunit to the KCNQ1 channel. *J Physiol* **542**, 119–130.

Grunnet M, Olesen SP, Klaerke DA & Jespersen T (2005). hKCNE4 inhibits the hKCNQ1 potassium current without affecting the activation kinetics. *Biochem Biophys Res Commun* **328**, 1146–1153.

Hong KH & Miller C (2000). The lipid–protein interface of a Shaker K^+ channel. *J General Physiol* **115**, 51–58.

Jiang Y, Lee A, Chen J, Cadene M, Chait BT & MacKinnon R (2002). The open pore conformation of potassium channels. *Nature* **417**, 523–526.

Jiang Y, Lee A, Chen J, Ruta V, Cadene M, Chait BT & MacKinnon R (2003). X-ray structure of a voltage-dependent K^+ channel. *Nature* **423**, 33–41.

Long SB, Campbell EB & Mackinnon R (2005). Crystal structure of a mammalian voltage-dependent Shaker family K^+ channel. *Science* **309**, 897–903.

McCrossan ZA & Abbott GW (2004). The MinK-related peptides. *Neuropharmacology* **47**, 787–821.

Melman YF, Domenech A, De La Luna S & McDonald TV (2001). Structural determinants of KvLQT1 control by the KCNE family of proteins. *J Biol Chem* **276**, 6439–6444.

Melman YF, Krumerman A & McDonald TV (2002). A single transmembrane site in the KCNE-encoded proteins controls the specificity of KvLQT1 channel gating. *J Biol Chem* **277**, 25187–25194.

Melman YF, Um SY, Krumerman A, Kagan A & McDonald TV (2004). KCNE1 binds to the KCNQ1 pore to regulate potassium channel activity. *Neuron* **42**, 927–937.

Mercer EA, Abbott GW, Brazier SP, Ramesh B, Haris PI & Srai SK (1997). Synthetic putative transmembrane region of minimal potassium channel protein (minK) adopts an alpha-helical conformation in phospholipid membranes. *Biochem J* **325**, 475–479.

Monks SA, Needleman DJ & Miller C (1999). Helical structure and packing orientation of the S2 segment in the Shaker K^+ channel. *J General Physiol* **113**, 415–423.

Sanguinetti MC, Curran ME, Zou A, Shen J, Spector PS, Atkinson DL & Keating MT (1996). Coassembly of K_VLQT1 and minK (IsK) proteins to form cardiac I_{Ks} potassium channel. *Nature* **384**, 80–83.

Schroeder BC, Waldegger S, Fehr S, Bleich M, Warth R, Greger R & Jentsch TJ (2000). A constitutively open potassium channel formed by KCNQ1 and KCNE3. *Nature* **403**, 196–199.

Seebohm G, Westenskow P, Lang F & Sanguinetti MC (2005). Mutation of colocalized residues of the pore helix and transmembrane segments S5 and S6 disrupt deactivation and modify inactivation of KCNQ1 K^+ channels. *J Physiol* **563**, 359–368.

Sesti F & Goldstein SA (1998). Single-channel characteristics of wild-type IKs channels and channels formed with two minK mutants that cause long QT syndrome. *J General Physiol* **112**, 651–663.

Tai KK & Goldstein SA (1998). The conduction pore of a cardiac potassium channel. *Nature* **391**, 605–608.

Tai KK, Wang KW & Goldstein SA (1997). MinK potassium channels are heteromultimeric complexes. *J Biol Chem* **272**, 1654–1658.

Takumi T, Ohkubo H & Nakanishi S (1988). Cloning of a membrane protein that induces a slow voltage-gated potassium current. *Science* **242**, 1042–1045.

Teng S, Ma L, Zhen Y, Lin C, Bahring R, Vardanyan V, Pongs O & Hui R (2003). Novel gene hKCNE4 slows the activation of the KCNQ1 channel. *Biochem Biophys Res Commun* **303**, 808–813.

Tinel N, Diochot S, Borsotto M, Lazdunski M & Barhanin J (2000). KCNE2 confers background current characteristics to the cardiac KCNQ1 potassium channel. *EMBO J* **19**, 6326–6330.

Tristani-Firouzi M & Sanguinetti MC (1998). Voltage-dependent inactivation of the human K^+ channel KvLQT1 is eliminated by association with minimal K^+ channel (minK) subunits. *J Physiol* **510**, 37–45.

Wang KW, Tai KK & Goldstein SA (1996*a*). MinK residues line a potassium channel pore. *Neuron* **16**, 571–577.

Wang Q, Curran ME, Splawski I, Burn TC, Millholland JM, VanRaay TJ *et al.* (1996*b*). Positional cloning of a novel potassium channel gene: KVLQT1 mutations cause cardiac arrhythmias. *Nat Genet* **12**, 17–23.

Yang WP, Levesque PC, Little WA, Conder ML, Shalaby FY & Blanar MA (1997). KvLQT1, a voltage-gated potassium channel responsible for human cardiac arrhythmias. *Proc Natl Acad Sci U S A* **94**, 4017–4021.

Yang Y & Sigworth FJ (1998). Single-channel properties of IKs potassium channels. *J General Physiol* **112**, 665–678.

Acknowledgements

G.W.A. is supported by the American Heart Association (0235069 N) and the National Institutes of Health (R01 HL079275; RO3 DC07060). We thank Earl Gordon and Dr Torsten Roepke for thoughtful comments on the manuscript.

Supplemental material

The online version of this paper can be accessed at:
DOI: 10.1113/jphysiol.2005.100644
http://jp.physoc.org/content/vol0/issue2005/images/data/jphysiol.2005.100644/DC1/Supfigandlegend.jpg
and contains supplemental material entitled:
Reciprocal mutagenesis for S338/V72 MiRP2 interaction.
This material can also be found as part of the full-text HTML version available from http://www.blackwell-synergy.com